Liquid Crystals
Publication details, including instructions for authors and subscription information:
http://www.informaworld.com/smpp/title~content=t713926090

X-ray study of the nematic and smectic A phases of the cyano-substituted pyridines

B. I. Ostrovskii[a]; A. I. Pavluchenko[b]; V. F. Petrov[b]; M. A. Saidachmetov[a]
[a] Institute of Crystallography, U. S. S. R. Academy of Sciences, Moscow, U.S.S.R. [b] Organic Intermediates and Dyes Institute, Moscow, U.S.S.R

To cite this Article Ostrovskii, B. I. , Pavluchenko, A. I. , Petrov, V. F. and Saidachmetov, M. A.(1989) 'X-ray study of the nematic and smectic A phases of the cyano-substituted pyridines', Liquid Crystals, 5: 2, 513 — 524
To link to this Article: DOI: 10.1080/02678298908045401
URL: http://dx.doi.org/10.1080/02678298908045401

LIQUID CRYSTALS, 1989, VOL. 5, NO. 2, 513–524

X-ray study of the nematic and smectic A phases of the cyano-substituted pyridines

by B. I. OSTROVSKII†, A. I. PAVLUCHENKO‡, V. F. PETROV‡ and M. A. SAIDACHMETOV†

†Institute of Crystallography, U.S.S.R. Academy of Sciences, Leninsky prospekt 59, Moscow 117333, U.S.S.R.

‡Organic Intermediates and Dyes Institute, B. Sadovaya 1-4, Moscow 103787, U.S.S.R.

We report an X-ray study of lamellar ordering in the nematic and smectic A phases of a homologous series of polar liquid crystals, the 2-(4-alkylphenyl)-5-cyanopyridines (*n*CP). Experiments were carried out using a diffractometer with a linear position sensitive detector. In the nematic and smectic A phases of the *n*CP and their mixtures with non-polar 4-*n*-butyl-4′-methoxyazoxybenzene two types of layering were found. One corresponds to the fluctuations of the smectic density wave with a monolayer wavevector q_1, and the other is due to the partial bilayer fluctuations with the incommensurate wavevector $q_2 \neq q_1/2$. The temperature dependences of the X-ray scattering intensity and the longitudinal correlation length for both types of layering in the nematic phase are presented. The critical behaviour in the vicinity of the smectic A–nematic phase transition occurs for a fluctuation mode, either q_1 or q_2, depending on the position on the liquid crystal phase diagram. The influence of the molecular structure of cyano-substituted pyridines on the formation of layered structures of different types is also discussed.

1. Introduction

Liquid crystals consisting of molecules with strongly polar end groups (–CN, –NO_2) exhibit a variety of lamellar packings [1–5]. Apart from the ordinary smectic A_1 phase with a spatial period, d, approximately equal to the molecular length, L, there are bilayered smectics A_2 with the period $d \approx 2L$ and intermediate (partial bilayered) smectics A_d whose spatial period is incommensurate with the molecular length $L < d < 2L$. In addition, a smectic $\tilde{A}$ phase has been observed with the density wave modulated along the direction perpendicular to the director $\mathbf{n}$. The existence of a smectic A_{ic} phase with two colinear incommensurate density waves has also been reported [6]. In phase diagrams of polar liquid crystals and their mixtures with non-polar compounds, phase transitions lines between the smectic A_1, A_2 and A_d phases can be observed, as well as between them and the nematic phase, including some re-entrant points. The symmetry of the phases S_{A_1}, S_{A_2}, S_{A_d} is the same, thus, the phase boundaries along which the S_{A_d} and S_{A_2} or S_{A_1} phases coexist can terminate at a critical point similar to the gas–liquid critical point [7, 8].

These phenomena are due to the specific nature of intermolecular interactions in polar liquid-crystalline compounds, resulting in various effects of molecular association. Anti-parallel correlations between permanent and induced molecular dipoles influence the subtle balance between the attractive dispersion forces and the repulsive steric ones, and give rise to the structural packing of the S_{A_1}, S_{A_2} or S_{A_d} types [9].

0267–8292/89 $3.00 © 1989 Taylor & Francis Ltd

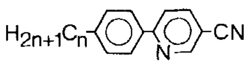

Figure 1. Molecular structure of the *n*CP homologous series, $n = 3$ and 5–7.

The molecular flexibility of the alkyl chains also influences the stability of the multiple S_A phases [10]. Simultaneously a phenomenological theory describing the formation of different density waves in the S_A phases has been developed, based on a free energy expression with two coupled smectic order parameters [4]. This model introduces the idea of frustrated smectics with competing length scales.

X-ray scattering is very sensitive to any change in lamellar packing of liquid crystals. In the nematic phase the small angle X-ray scattering is concentrated near vectors $q_i = 2\pi/l_i$ in reciprocal space. Here l_i is the length of the structural unit of the medium which may often be referred to as a molecular associate. The intensity of the X-ray scattering from the nematic phase includes two additional contributions against the isotropic background. The first, pure nematic, results from the orientational correlations of the long molecular axes, the second is due to the scattering by smectic fluctuations in the nematic phase. The latter contribution to intensity increases anomalously near the transition into the smectic A phase. Evidently, a variety of smectic phases influences the fluctuational behaviour in the nematic phase. This means that X-ray scattering allows the nucleation of different smectic phases in the nematic phase to be studied at the level of fluctuations.

Here results are reported of X-ray investigations of lamellar ordering in the nematic and smectic A phases for a homologous series of polar liquid crystals, the 2-(4-alkylphenyl)-5-cyanopyridines (*n*CP); their molecular structures are shown in figure 1. The synthesis and various physico-chemical properties of the cyano-substituted pyridines have been reported earlier [11]. The influence of the nitrogen in the pyridine moiety on the structure of the liquid-crystalline phases has been analysed by Petrov *et al.* [12].

2. Experimental technique

X-ray investigations were carried out using a diffractometer with a linear position sensitive detector which records simultaneously a diffraction pattern over a wide range of scattering angles (see figure 2). In different experiments an X-ray beam (Cu*Kα* radiation) was formed with either a three slit collimation scheme with a

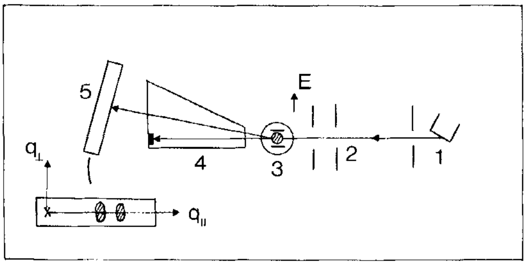

Figure 2. X-ray diffractometer with a linear position sensitive detector. 1, X-ray tube; 2, vertical collimation slits; 3, sample in a thermostat; 4, vacuum tube; 5, detector. The inset shows the detector window, the cross denotes the direct beam, $q_\parallel$ and $q_\perp$ are the wavevector components in the direction collinear with and normal to the director **n**; hatched area is a scattering distribution in a plane of the detector.

nickel-filter or by using a crystal monochromator [13]. The scattered radiation passed through a vacuum chamber. The spatial resolution of the detector was 0·13 mm. With the sensitive area for the detector of 10 × 50 mm^2 and the distance between the specimen and the detector of 450 mm a diffraction pattern was detected in the angular range from 0 to 6° with a resolution of 0·015°. The instrumental function was approximated by a gaussian whose width at a half height $\Delta(2\theta)$ varied from 0·03 to 0·1° depending on the beam formation scheme (2θ is the scattering angle). The instrumental function was recorded using a standard sample, oriented 4-*n*-octyl-4′-cyanobiphenyl (8CB) in the smectic A phase which provides a narrow scattering line [14]. Depending on the experimental conditions the exposure time was varied from 100 to 1000 s. The scattering intensities were recorded (point-by-point with a step of 0·01°) and were analysed. The window of the detector was placed in the detection plane in a way which allowed the reconstruction of the scattering pattern of a nematic along the $q_{\parallel}$ coordinate in reciprocal space; that is, along the direction parallel to the detector, **n**. In the experiments the intensity, angular position and width (in the nematic phase) of the diffraction maxima were measured. A thermostat was used, with the liquid crystal set in the reflecting position. Samples with dimensions 1·5 × 1·5 × 2 mm^3 were placed between plane electrodes. The director was oriented by an A.C. electric field (frequency 3 kHz, field strength 1 kV cm^{-1}). Such a field was sufficient to achieve complete orientation of the director because of the large dielectric anisotropy ($\Delta\varepsilon \approx 10$) of the substance. The temperature was measured with a calibrated thermistor and was stable to an accuracy of 0·01 K.

3. X-ray scattering from nematic liquid crystals

For an anisotropic liquid the intensity of X-ray scattering is given by [15]

$$I(\mathbf{q})/I_0 = \varrho^2 \int \langle F(\mathbf{q}, \omega_1) \cdot F(\mathbf{q}, \omega_2)\, G(\mathbf{r}_{12}, \omega_1, \omega_2)\rangle_{\omega_1,\omega_2} \exp(i\mathbf{q}\mathbf{r}_{12})\, d\mathbf{r}_{12} \qquad (1)$$

where ϱ is the number density, $F(\mathbf{q}, \omega)$ is the structural amplitude for particles with orientation ω, $G(\mathbf{r}_{12}, \omega_1, \omega_2)$ is a pair correlation function depending on both the distance between the centres of gravity and the mutual orientation of the particles, $q = (4\pi/\lambda)\sin\theta$ is the scattering vector. In the nematic phase the intensity $I(\mathbf{q})$ is predetermined by the long range orientational order of the long molecular axes and the short range (liquid-like) order in position of the molecular centres ($I_N(\mathbf{q})$ is the nematic contribution to the total intensity). The specific feature of nematic liquid crystals is the dependence of the intermolecular distance of the mutual orientation of neighbour molecules. Hence, in the pair correlation function $G(\mathbf{r}_{12}, \omega_1, \omega_2)$ apart from correlations of the position–position and orientation–orientation types mixed correlations of the position–orientation type have to be considered. The influence of the latter on the viscoelastic properties of liquid crystals has been analysed by Van der Meer *et al.* (i.e. the so-called smectic-like correlations) [16]. There is some evidence that these correlations play an important role in liquid crystals where molecular association occurs [17].

In the vicinity of the transition to the smectic A phase the long wavelength positional correlations along the director begin to play an increasing role in the correlation function, $G(\mathbf{r}_{12}, \omega_1, \omega_2)$. This is a consequence of the appearance of fluctuating domains with smectic order. The density change corresponding to one dimensional positional order along the director **n** (i.e. the z axis) is

$$\delta\varrho = \mathrm{Re}\,[\psi \exp(iq_0 z)], \qquad (2)$$

where ψ is the parameter for the smectic A–nematic transition ($q_0 = 2\pi/d$, d being the layer spacing). In the nematic phase, where $\langle\psi\rangle = 0$ X-ray scattering takes place from fluctuations in the parameter ψ, i.e. from domains with smectic ordering with characteristic correlation lengths $\xi_\parallel$ and $\xi_\perp$ parallel and perpendicular to the director. This additional scattering is proportional to the correlator of the smectic fluctuations $\langle\psi^2(\mathbf{q})\rangle$ which, in the Ornstein–Zernike approximation, has the form [18]

$$\langle\psi^2(\mathbf{q})\rangle = \frac{kT\chi}{1 + \xi_\parallel^2(q_\parallel - q_0)^2 + q_\perp^2\xi_\perp^2}. \tag{3}$$

Here χ is the generalized susceptibility which describes the response of the layered structure to external factors. Using equation (3) we can calculate the magnitude of the longitudinal correlation length $\xi_\parallel \approx \lambda/\Delta(2\theta)$ from the angular width of the intensity profile at the half-height $\Delta(2\theta)$.

For a liquid crystal consisting of polar molecules there are two competing lengths; namely, the molecular length and length of the antiparallel dipolar pairs L', $L < L' < 2L$ [4]. The X-ray diffraction spectrum from the nematic phase shows scattering in the vicinity of two wavevectors $q_1 = 2\pi/L$ and $q_2 = 2\pi/L'$; these correspond to scattering from fluctuational smectic modes of the S_{A_1} and S_{A_d} types:

$$I(\mathbf{q}) = I_N(\mathbf{q}) + I_{S_1}(\mathbf{q}) + I_{S_\alpha}(\mathbf{q}). \tag{4}$$

As the line of phase transitions into S_{A_1} or S_{A_d} phases is approached, critical enhancement of scattering occurs for that fluctuation mode which is thermodynamically stable in the corresponding A phase. Thus, X-ray scattering in the nematic phase provides information on both the types of structural units of medium (monomers, dimers, etc.) and on the type of thermodynamically preferred lamellar ordering.

4. Experimental results and interpretation

The phase diagram for a homologous series of *n*CP is shown in figure 3. The smectic A phase appears beginning with the sixth homologue. By using mixtures of the homologues 6CP and 5CP we can specify the position of both the crystallization

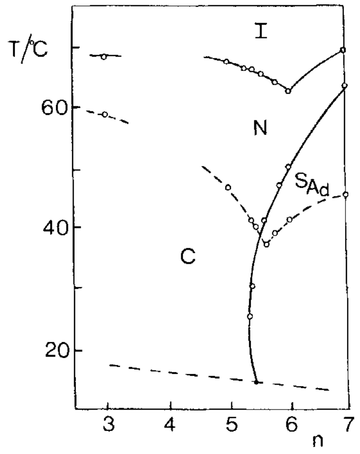

Figure 3. Phase diagram for the homologous series of the *n*CP. The broken curves correspond to crystal–nematic and conjectural monotropic smectic A_1–nematic A phase boundaries.

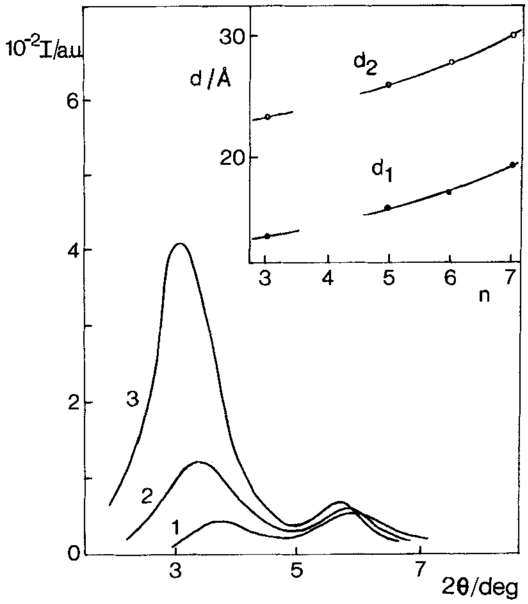

Figure 4. X-ray diffraction patterns corresponding to coexistence of the layer structures of monolayer (d_1) and partial bilayer (d_2) types in the nematic phase of the *n*CP homologous series. 1, 3CP; 2, 5CP; 3, 6CP; $T - T_{NI} = 4°C$. The inset shows the variation of the layer spacing, *d*, for the *n*CP.

line and the smectic A–nematic transition. For $x > 0{\cdot}5$ (where x is the concentration of 5CP in a 5CP–6CP mixture) the S_A–N line crosses the crystallization line and the smectic A phase becomes monotropic. For the whole homologous series of *n*CP X-ray scattering from the smectic density waves of different types (periods d_1 and d_2 in figure 4) can be observed. With increasing homologue number the lamellar packing of the monomeric type, $d_1 \approx L$, becomes more unstable and the dimeric mode, corresponding to partly overlapped molecules, $L < d_2 < 2L$, becomes more pronounced in the scattering spectra (see figures 4 and 5).

For concentrations of the 5CP component $x < 0{\cdot}6$ the scattering intensity due to the fluctuations of the dimer density wave increases strongly (see figure 5(*b*)). This may be accounted for by the fact that the line of the experiment ($T - T_{NI} \approx 4°$) at the phase diagram approaches the line of the S_A–N transition. The scattering from the monomeric density wave in the same concentration–temperature range decreases and then passes through a minimum at $x = 0{\cdot}2$ (see figure 5(*a*)). The temperature dependences of the layer spacings d_1 and d_2 in the nematic and smectic A phases for 5CP and 6CP are shown in figure 6. In 6CP the S_{A_d} layer spacing increases monotonically as the nematic–smectic transition is approached from above and then remains constant. The smectic A_1 spacing shows a dramatic decrease at the S_{A_d}–N transition. In 5CP d_2 decreases slightly with temperature, while d_1 remains unchanged. This difference in the temperature behaviour of the layer spacing of the two compounds is probably due to the different role of molecular dimers in the formation of layers and will be discussed later.

In 6CP in both the nematic and smectic A phase we have observed scattering in the vicinity of two vectors of reciprocal space, namely, $q_1 \approx 0{\cdot}35\,Å^{-1}$ characteristic of the layered structure with a period $d_1 \approx L$, and $q_2 \approx 0{\cdot}22\,Å^{-1}$ corresponding to the

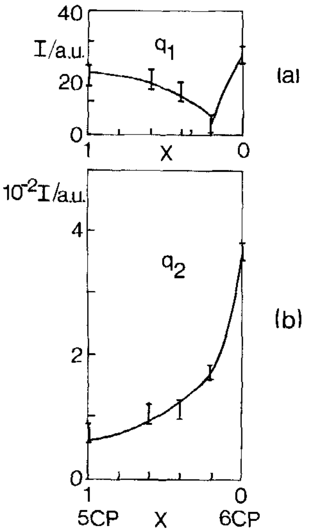

Figure 5. X-ray scattering intensity at (*a*) monolayer q_1 and (*b*) partial bilayer q_2 wavenumbers versus concentration in the nematic phase for 5CP–6CP mixture; x is the concentration of 5CP, $T - T_{NI} \approx 4°C$.

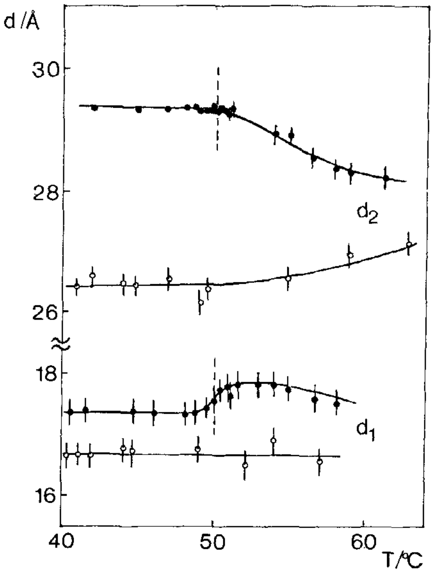

Figure 6. Temperature dependence of the layer spacing, d, at the monolayer (d_1) and partial bilayer (d_2) density waves in a nematic and smectic A (6CP) phases for (○) 5CP and (●) 6CP.

density wave with a period larger than the molecular length, $d_2 \approx 1{\cdot}5L$. At q_1 the scattering intensity is almost independent of temperature whereas the q_2 intensity increases anomalously when approaching the smectic A–nematic transition (see figure 7). Thus, in the smectic A phase of 6CP the density wave of the S_{A_d} type is thermodynamically stable. The temperature dependence of the longitudinal

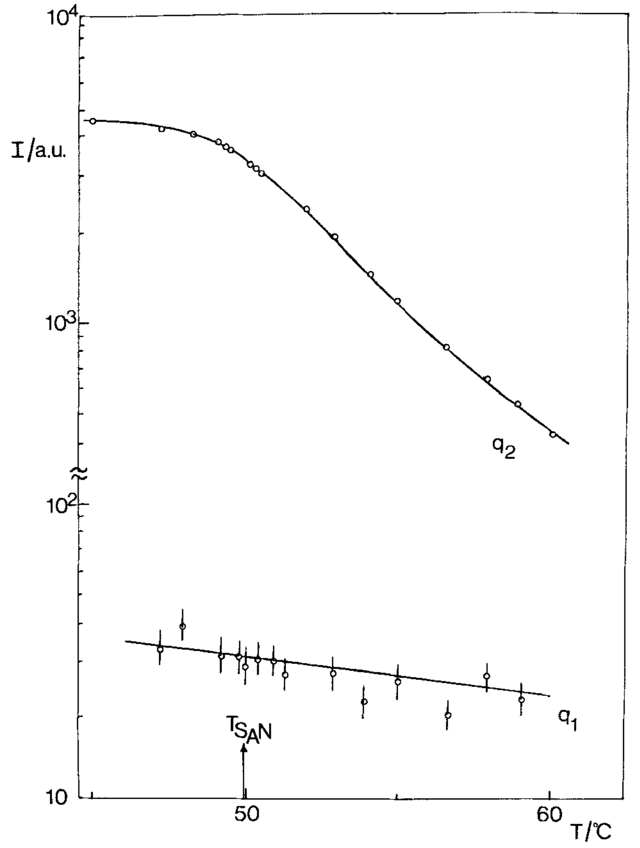

Figure 7. X-ray scattering intensity at the monolayer (q_1) and partial bilayer (q_2) wavenumbers versus temperature in the nematic and smectic A phases for 6CP.

correlation length for the q_2 wave is well described by the expression

$$\xi_{\|2} = \xi_{\|20}\tau^{-\nu_{\|}},$$

where $\tau = T - T_c/T_c$ is the reduced temperature (see figure 8). The values of critical exponent $\nu_{\|} = 0{\cdot}75 \pm 0{\cdot}05$ and the bare correlation length $\xi_{\|20} \approx 6{\cdot}9$ Å agree well with those for liquid crystals having approximately the same nematic width. The magnitude of the longitudinal correlation length for the q_1 wave $\xi_{\|1} \approx 80$ Å is several times more then the molecular length ($L \approx 20$ Å), however it is in fact, temperature independent. Similar results were obtained for the three mixtures of 5CP and 6CP with concentrations $x = 0{\cdot}2$, $0{\cdot}4$ and $0{\cdot}6$. The longitudinal correlation lengths were fitted to simple power laws and the critical exponents $\nu_{\|} = 0{\cdot}75$–$0{\cdot}78$, similar to those of pure 6CP, were obtained. The bare correlation lengths $\xi_{\|20}$ for these mixtures increase with increasing 5CP concentration from $\xi_{\|20} \approx 9{\cdot}4$ Å ($x = 0{\cdot}2$) to $\xi_{\|20} \approx 14°$ ($x = 0{\cdot}6$). For the two mixtures with $x = 0{\cdot}4$ and $0{\cdot}6$ the fit to simple power laws was rather poor for the reduced temperature range $\tau \gtrsim 10^{-2}$. In order to understand the results obtained for 5CP–6CP mixtures, we must account for the effect of the curvature in the smectic A–nematic phase boundary on the observed divergences (see figure 3). The crossover effects connected with the non-linear phase boundaries are

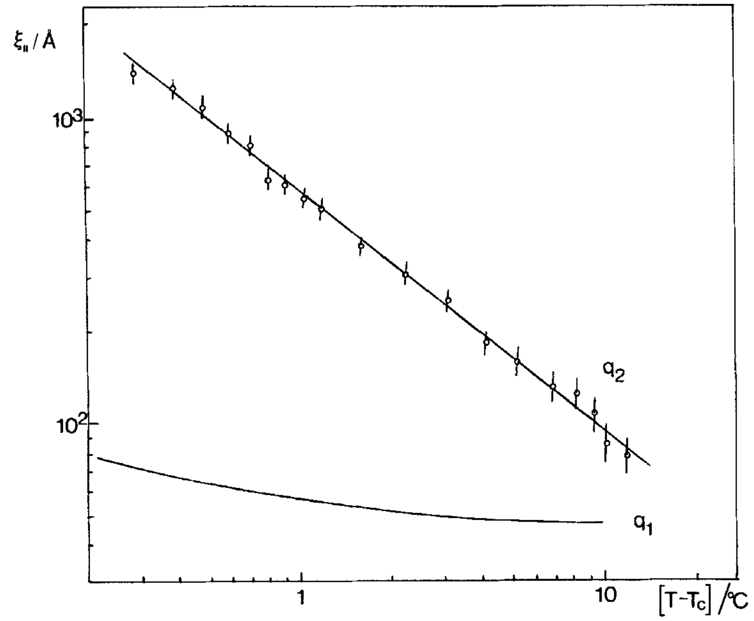

Figure 8. Longitudinal correlation length of the monolayer ($\xi_{\parallel 1}$) and bilayer ($\xi_{\parallel 2}$) formation versus temperature on a double logarithmic scale for 6CP.

well pronounced when the $S_{A\leftrightarrow N}$ transition curve lies in vicinity of either the re-entrant point [19] or the multicritical NAC point [20]. Least-squares analysis indicates that the S_{A_d}–N transition curve has a parabolic form in the T, X coordinates ($x = 0$–$0{\cdot}66$) for the 5CP–6CP mixture,

$$(T_M - T)^2 + \alpha(x - x_0) = 0,$$

with a median temperature $T_M \approx 295$ K and a critical concentration $x_0 \approx 0{\cdot}66$. In this case the correlation length takes the form [19]

$$\xi_\parallel = cT^{-\nu_\parallel}(\tau + T_c/\Delta T\tau^2)^{-\nu_\parallel},$$

where ΔT is the smectic A range and c is a constant. This equation predicts the bare correlation length increases and the range of the simple power law behaviour of the correlation length $\tau \lesssim \Delta T/T_c$ decreases with $\Delta T \to 0$. These predictions are in good accord with our $\xi_{\parallel 2}$ data. The detailed analysis of the $\xi_{\parallel 2}$ divergences for the 5CP–6CP mixtures will be the subject of a special paper.

The measurements carried out for 5CP which does not have a smectic A phase showed that both $I(q)$ and $\xi_{\parallel 2}$ for dimeric density wave fluctuations increase with decreasing temperature, however, $\xi_{\parallel 2}$ does not behave critically (see figure 9). In this case, the growth of $\xi_{\parallel 2}$ is due to the specific feature of the phase diagram for the nCP series (see figure 3) as, in our experiment, with decreasing temperature the thermodynamic route approaches the line of the S_{A_d}–N transition. The correlation length $\xi_{\parallel 1}$ for fluctuations of the monomeric type in 5CP exceeds several times the molecular length, but its temperature dependence is less pronounced than with $\xi_{\parallel 2}$ (see figure 9). It is clearly seen from our X-ray data that 5CP is in a marginal position on the phase diagram of the nCP homologous series, between compounds with a tendency for the formation of S_{A_1} and S_{A_d} layers. It is confirmed by the fact that a rather small amount

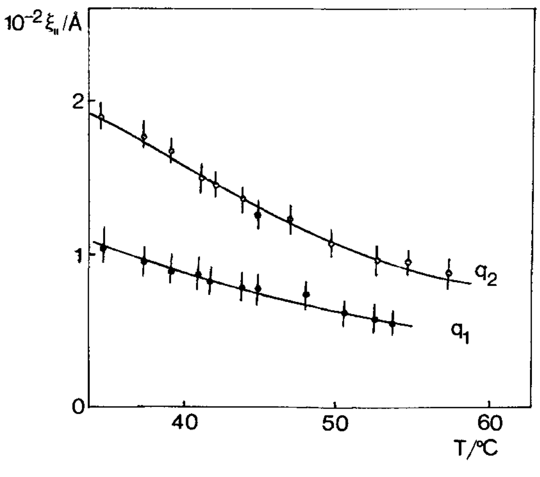

Figure 9. Longitudinal correlation length of the monolayer ($\xi_{\parallel 1}$) and bilayer ($\xi_{\parallel 2}$) formation versus temperature for 5CP.

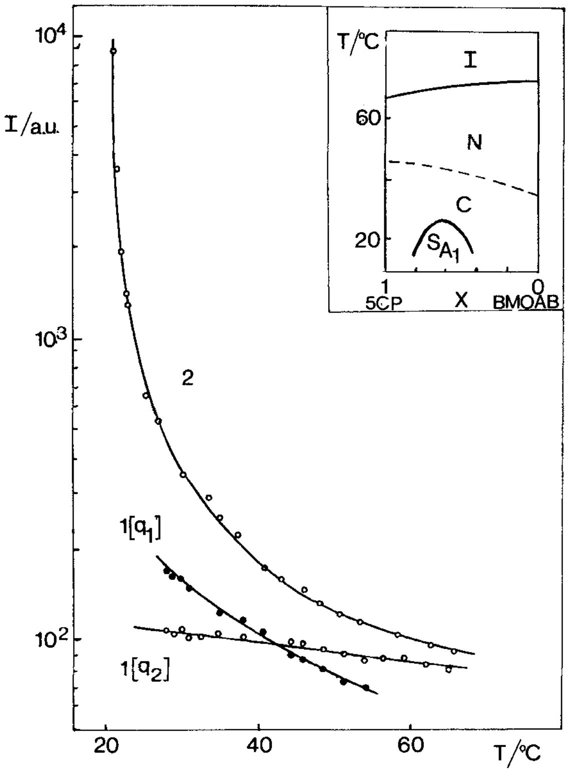

Figure 10. X-ray scattering intensity versus temperature in the nematic phase for certain concentrations x of the polar component 5CP in the mixture with BMOAB. 1, $x = 0{\cdot}8$, $d_1 = 17{\cdot}4$ Å, $d_2 = 24{\cdot}5$ Å; 2, $x = 0{\cdot}7$, $d_1 = 17{\cdot}8$ Å, $T_{S_{A_1}N} = 21{\cdot}4$°C. For the concentration $x = 0{\cdot}8$ X-ray scattering shows both monolayer (q_1) and partial bilayer (q_2) layering. The inset shows the 5CP–BMOAB phase diagram.

of the non-polar 4-*n*-butyl-4′-methoxyazoxybenzene (BMOAB) mixed with 5CP induces a smectic A_1 phase (see figure 10). The temperature dependence of the longitudinal correlation length for the q_1 wave is well described by the simple power law

$$\xi_{\parallel 1} = \xi_{\parallel 10}\tau^{-\nu_{\parallel}}$$

with the values of the critical exponent $\nu_{\parallel} \approx$ 0·67–0·70 and the bare correlation length $\xi_{\parallel 10} \simeq$ 9·5–10·5 Å.

5. Discussion

The results obtained for the *n*CP series point to the existence in the nematic phase of associates (dimers) of the cyanopyridine molecules due to dipole–dipole correlations. In this case smectic fluctuations with period d_2 correspond to the lamellar packing of the dimer and d_2 is the length of the *n*CP dimer. The change in the character of the associations in a homologous series of *n*CP may probably be explained by the specific dipolar structure of the *n*CP molecules. Conjugation of the CN dipole with an aromatic ring leads to delocalization of the dipole over the entire conjugated part of the molecule [21, 22]. The degree of overlap of two monomers when forming a dimer depends on the degree of conjugation (charge separation) and the geometrical anisotropy of the molecule. In the *n*CP compounds the CN dipole moment and the longitudinal dipole component of the pyridine moiety are directed on opposite sides, hence, the charge separation is partially decreased compared with the cyanobiphenyl derivatives, and so the antiparallel dipolar correlations become weaker. This is confirmed by the fact that dimer period, d_2, in 5CP is larger (d_2 = 26·4 Å) than that for a member of the alkylcyanobiphenyl series (*n*CB), 5CB (d_2 = 24·8 Å [23]), with the length of individual molecules being equal (L = 18·5 Å). Consequently the effects of bilayer formation are less pronounced in the *n*CP than in the *n*CB series. Such behaviour is typical of the series of three-ring compounds with terminal polar groups, where members with small alkyl (alkyloxy) chains have a tendency to form a monolayer S_{A_1} phase at low temperatures [3].

In order to understand the reason for the formation of the smectic A_d phase in the *n*CP series it is useful to analyse the temperature changes in the interlayer distance d_2 (see figure 6). In liquid-crystalline systems, where a dynamic equilibrium occurs between monomer and dimer numbers (D ⇄ 2M), the sign of the derivative $\partial d_2/\partial T$ is governed unambiguously by the temperature behaviour of the ratio $N/N + M$, where N is a number of dimers and $N + M$ is the total number of molecules in both monomer and dimer states. It results from the relationship between the interlayer distance and the dimer concentration X_D [24]

$$d_2 = L_D X_D + (1 - X_D)L_M,$$

where L_D and L_M are the dimer and monomer molecular lengths, respectively. This formula has been used for the interpretation of the behaviour of d_2 in re-entrant nematics [24] and nematic mixtures of strongly and weakly polar compounds [23, 25].

Thus, the increase of the interlayer distance, d_2, in 6CP as the S_{A_d}–N transition is approached from above (see figure 6) may be accounted for by an increase in the dimer concentration. For 5CP the d_2 value decreases only slightly with temperature, indicating the temperature independence of the dimer concentration. Such behaviour correlates with the absence of a smectic A–nematic transition in 5CP. The results obtained for 5CP–6CP mixtures confirm the approach to the description of the smectic–nematic transition in systems consisting of polar molecules as to the transition of the percolation type [21, 26]. Such a transition occurs at a certain concentration of dimers in a liquid crystal. For polar molecules with relatively short alkyl or alkoxy chains the percolation model explains the formation of the smectic A_d phase by sufficiently large number of dimers with the more favourable (than for monomers) MacMillan ratio when the length of the rigid molecular core decreases with respect to the total length of a dimer.

As to the formation of an induced smectic A_1 phase in the mixture of 5CP with the non-polar BMOAB, the nature of this A_1 phase is not clear. The addition of BMOAB to polar 5CP shifts the dynamic equilibrium $D \rightleftarrows 2M$ in the direction of decreasing of dimer concentration, since the probability of the formation of a mixed associate between molecules of 5CP and BMOAB by means of a dipole-induced dipole interaction is less than the probability of the formation of a dimer from two polar 5CP molecules. In this situation the greater stability of smectic A_1 phase than that of pure compounds can be caused by the formation of electron-donor–acceptor (EDA) complexes by molecules with different electronic properties [27].

The results obtained for the *n*CP homologous series indicate clearly that the alkyl chain length affects the tendency to form smectic A phases of different types. For the higher homologues ($\gtrsim C_5$) the dimeric layer organization is more stable than for the lower members. The length of the alkyl chain has no influence on the degree of conjugation of the molecule [21, 22], hence it can affect the stability of smectic phases via packing effects. This may be discussed qualitatively as follows. The *n*-alkyl chains are semiflexible in the liquid-crystalline state since the energy to make a *trans–gauche* rotation about any carbon–carbon bond is comparable to thermal energies. With decreasing temperature the *trans–gauche* isomerization becomes less probable, so that in a crystalline state the aliphatic chains are in the all-*trans* state. Higher homologues have more possibilities for *gauche* conformers, and some of these may be energetically favoured depending on the temperature, the structure of the rigid core and the degree of molecular overlapping in the associates. The partial bilayer smectics, being loose in the aliphatic tail regions, are very sensitive to any effects caused by changes in the packing entropy. The higher homologous can give a denser packing in the S_{A_d} phase even for a large concentration of dimers at sufficiently high temperatures, where their conformational ability is high. For lower homologues or for sufficiently low temperatures, where molecules are mainly in the all-*trans* conformation the unfavourable packing of the aliphatic chains can cause the transition to either the monolayer smectic A_1 or the nematic phase. The numerical results obtained by Dowell [10] in her recent work where the chain flexibility was shown to play an important role in the stability of multiple smectic A phases, confirm this assumption.

In our experiment we were not able to observe the monolayer A_1 phase for the *n*CP homologous series, but the scattering from the nematic phase shows diffuse peaks centred at the monolayer wavevector q_1 (see figures 4, 5 and 7). The width of the q_1 scattering curve is indicative of longitudinal correlations of about 60–100 Å, i.e. between three and five molecular lengths (see figures 8 and 9). The correlation length $\xi_{\parallel 1}$ for monomeric fluctuations increases slightly in 5CP when the temperature is lowered (see figure 9) displaying the proximity of the low temperature nematic phase to the line of the S_A–N transition. Unfortunately, the S_{A_1}–N transition line is totally inaccessible for the *n*CP series because of crystallization. A possible reconstruction of the monotropic smectic A_1–nematic line for the *n*CP series is shown in figure 3.

The observed minimum of the X-ray intensity at the monolayer wavenumber q_1 at a concentration of 5CP in 6CP of $X = 0{\cdot}2$ (see figure 5(*a*)) may be connected with the existence of the monotropic multicritical NA_1A_d point in the phase diagram of the *n*CP series (see figure 3).

The authors are grateful to Professor L. M. Blinov for his interest to this work, D. A. Goganov and S. M. Gutkevich for their help with the detector, and to M. A. Averyanov, M. F. Grebyonkin and M. A. Osipov for fruitful discussions.

References

[1] Levelut, A. M., Tarento, R. J., Hardouin, F., Achard, M. F., and Sigaud, G., 1981, *Phys. Rev.* A, **24**, 2180.
[2] Brownsey, G. I., and Leadbetter, A. J., 1980, *Phys. Rev. Lett.*, **44**, 1608.
[3] Hardouin, F., Levelut, A. M., Achard, M. F., and Sigaud, G., 1983, *J. Chim. Phys.*, **80**, 53.
[4] Prost, J., and Barois, P. 1983, *J. Chim. Phys.*, **80**, 65.
[5] De Jeu, W. H., 1986, *Structural Incommensurability in Crystals, Liquid Crystals and Quasi-crystals*, edited by J. F. Scott (Plenum Press).
[6] Ratna, B. R., Shashidhar, R., and Raja, V. N., 1985, *Phys. Rev. Lett.*, **55**, 1476.
[7] Hardouin, F., 1986, *Physica* A, **140**, 359.
[8] Shashidhar, R., Ratna, B. R., Prasad Krishna, S., Somasekhara, S., and Heppke, G., 1987, *Phys. Rev. Lett.*, **59**, 1209.
[9] Indekeu, J. O., and Berker, A. N., 1986, *Physica* A, **140**, 368.
[10] Dowell, F., 1987, *Phys. Rev.* A, **36**, 5046.
[11] Grebyonkin, M. F., Petrov, V. F., Belyaev, V. V., Pavluchenko, A. I., Smirnova, N. I., Kovshev, E. I., Titov, V. V., and Ivashenko, A. V., 1985, *Molec. Crystals liq. Crystals*, **129**, 245.
[12] Petrov, V. F., Grebyonkin, M. F., and Ostrovskii, B. I., 1988, *Kristallogrfiya*, **33**, 1194.
[13] L'vov, Yu. M., Ostrovskii, B. I., and Feigin, L. A., 1987, *Kristallografiya*, **32**, 972. (1987, *Soviet Phys. Crystallogr.*, **32**, 571).
[14] Zisman, A. N., Nikiforov, D. V., Ostrovskii, B. I., and Terent'ev, E. M., 1987, *Pis'ma Zh. eksp. teor. Fiz.*, **45**, 193. (1987, *JETP Lett.*, **45**, 238).
[15] Kopp, W., and Wendorff, J. H., 1982, *Coll. Polym. Sci.*, **260**, 1071.
[16] Van der Meer, B. W., Postma, F., Dekker, A. J., and de Jeu, W. H., 1982, *Molec. Phys.*, **45**, 1227.
[17] Bradshaw, M. J., Raynes, E. P., Fedak, I., and Leadbetter, A. J., 1984, *J. Phys. Paris*, **45**, 157.
[18] Litster, J. D., Als-Nielsen, J., Birgeneau, R. J., Dana, S. S., Davidov, D., Garsia-Golding, F., Kaplan, M., Safinya, C. R., and Schaetzing, R., 1979, *J. Phys. Paris, Coll.* C3, **40**, 339.
[19] Kortan, A. R., von Kanel, H., Birgeneau, R. J., and Litster, J. D., 1984, *J. Phys. Paris*, **45**, 529.
[20] Solomon, L., and Litster, J. D., 1986, *Phys. Rev. Lett.*, **56**, 2268.
[21] De Jeu, W. H., 1983, *Phil. Trans. R. Soc.* A, **309**, 217.
[22] Osman, M. A., 1983, *Z. Naturf.* (*a*), **38**, 779.
[23] Zeinalov, R. A., Blinov, L. M., Grebyonkin, M. F., Ostrovskii, B. I., and Saidachmetov, M. A., 1988, *Kristallografiya*, **33**, 185.
[24] Cladis, P. E., Guillon, D., Bouchet, F. R., and Finn, P. L., 1981, *Phys. Rev.* A, **23**, 2594.
[25] Blinov, L. M., Grebyonkin, M. F., Zeinalov, R. A., Ostrovskii, B. I., and Petrov, V. F., 1989, *Kristallografiya*, **34**, 398.
[26] Longa, L., and de Jeu, W. H., 1982, *Phys. Rev.* A, **26**, 1632.
[27] De Jeu, W. H., Longa, L., and Demus, D., 1986, *J. chem. Phys.*, **84**, 6410.